

The SCOLE Design Challenge

by

**Larry Taylor
NASA Langley
Research Center
and
A. V. Balakrishnan
U. C. L. A.**

JUNE 1984

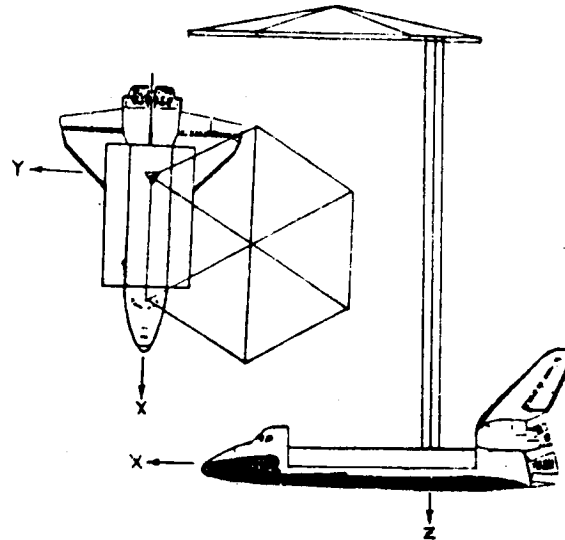
A MATHEMATICAL PROBLEM AND A SPACECRAFT CONTROL LABORATORY
EXPERIMENT (SCOLE) USED TO EVALUATE CONTROL LAWS FOR
FLEXIBLE SPACECRAFT... NASA/IEEE DESIGN CHALLENGE

by

Lawrence W. Taylor, Jr.
Spacecraft Control Branch
NASA Langley Research Center
Hampton, VA 23665

and

A. V. Balakrishnan
Chairman, IEEE Subcommittee on Large Space Structures, COLSS
System Sciences Department
University of California at Los Angeles
Los Angeles, CA



NASA

IEEE

A MATHEMATICAL PROBLEM AND A SPACECRAFT CONTROL LABORATORY
EXPERIMENT (SCOLE) USED TO EVALUATE CONTROL LAWS FOR
FLEXIBLE SPACECRAFT... NASA/IEEE DESIGN CHALLENGE

by

Lawrence W. Taylor, Jr.
Spacecraft Control Branch
NASA Langley Research Center
Hampton, VA 23665

and

A. V. Balakrishnan
Chairman, IEEE Subcommittee on Large Space Structures, COLSS
System Sciences Department
University of California at Los Angeles
Los Angeles, CA

SUMMARY

The problem of controlling large, flexible space systems has been the subject of considerable research. Many approaches to control system synthesis have been evaluated using computer simulation. In several cases, ground experiments have also been used to validate system performance under more realistic conditions. There remains a need, however, to test additional control laws for flexible spacecraft and to directly compare competing design techniques. In this paper an NASA program is discussed which has been initiated to make direct comparisons of control laws for, first, a mathematical problem, then an experimental test article is being assembled under the cognizance of the Spacecraft Control Branch at the NASA Langley Research Center with the advice and counsel of the IEEE Subcommittee on Large Space Structures. The physical apparatus will consist of a softly supported dynamic model of an antenna attached to the Shuttle by a flexible beam. The control objective will include the task of directing the line-of-sight of the Shuttle/antenna configuration toward a fixed

target, under conditions of noisy data, limited control authority and random disturbances. The open competition started in the early part of 1984. Interested researchers are provided information intended to facilitate the analysis and control synthesis tasks. A workshop is planned for early December at the NASA Langley Research Center to discuss and compare results.

INTRODUCTION

Many future spacecraft will be large and consequently quite flexible. As the size of antennae is increased, the frequencies of the first flexible modes will decrease and overlap the pointing system bandwidth. It will no longer be possible to use low gain systems with simple notch filters to provide the required control performance. Multiple sensors and actuators, and sophisticated control laws will be necessary to ensure stability, reliability and the pointing accuracy required for large, flexible spacecraft.

Control of such spacecraft has been studied with regard given to modeling, order reduction, fault management, stability and dynamic system performance. Numerous example applications have been used to demonstrate specific approaches to pertinent control problems. Both computer simulations and laboratory experiment results have been offered as evidence of the validity of the approaches to control large, flexible spacecraft. Concerns remain, however, because of the chronic difficulties in controlling these lightly damped large-scale systems. Because of these concerns and because of the desire to offer a means of comparing technical approaches directly, an NASA/IEEE Design Challenge is being offered. An

experimental test article is being assembled under the cognizance of the Spacecraft Control Branch at the NASA Langley Research Center with the advice and counsel of the IEEE (COLSS) Subcommittee on Large Space Structures. This Spacecraft Control Laboratory Experiment (SCOLE) will serve as the focus of a design challenge for the purpose of comparing directly different approaches to control synthesis, modeling, order reduction, state estimation and system identification.

The configuration of the SCOLE will represent a large antenna attached to the Space Shuttle orbiter by a flexible beam. This configuration was chosen because of its similarity to proposed space flight experiments and proposed space-based antenna systems. This paper will discuss the "Design Challenge" in terms of both a mathematical problem and a physical experimental apparatus. The SCOLE program is not part of any flight program.

SYMBOLS

| | |
|-------|---|
| a | acceleration vector ft/sec^2 |
| A | beam cross section area |
| c | observation matrix |
| d | noise contaminating direction cosine matrix measurements |
| e | line-of-sight error |
| E | modulus of elasticity |
| f | concentrated force expressions |
| F_4 | force vector |
| g | concentrated moment expressions |
| GI | torsional rigidity |
| I | moment of inertia matrix for entire Shuttle/antenna configuration |

| | |
|------------|--|
| I_1 | moment of inertia matrix, Shuttle body |
| I_4 | moment of inertia matrix, reflector body |
| I_ϕ | beam cross section moment of inertia, roll bending |
| I_θ | beam cross section moment of inertia, pitch bending |
| I_ψ | beam polar moment of inertia, yaw torsion |
| L | length of the reflector mast, beam |
| M_1 | control moment applied to the Shuttle body |
| M_4 | control moment applied to the reflector body |
| M_D | disturbance moment applied to the Shuttle body |
| m | mass of entire Shuttle/antenna configuration |
| m_1 | mass of Shuttle body |
| m_4 | mass of reflector body |
| P | mass density of beam |
| s | beam position variable |
| T_1 | direction cosine matrix, Shuttle body $()_{\text{earth}} = T_1 ()_{\text{Shuttle body}}$ |
| T_4 | direction cosine matrix, reflector body $()_{\text{earth}} = T_4 ()_{\text{reflector body}}$ |
| v_1 | inertial velocity, Shuttle body |
| v_4 | inertial velocity, reflector body |
| u_ϕ | lateral deflection of beam bending in y-z plane |
| u_θ | lateral deflection of beam bending in x-z plane |
| u_ψ | angular deflection of beam twisting about z axis |
| X, Y, Z | position variables |
| Δ | displacement of proof-mass actuator |
| δ | line-of-sight pointing requirement |
| ϵ | noise contaminating angular velocity measurements |

| | |
|----------------------|---|
| θ, ϕ, ψ | pitch, roll, heading |
| ζ | damping ratio |
| τ | noise contaminating acceleration measurements |
| ω_1 | angular velocity of Shuttle body |
| ω_4 | angular velocity of reflector body |

DISCUSSION

The objective of the NASA-IEEE Design Challenge concerning the control of flexible spacecraft is to promote direct comparison of different approaches to control, state estimation and systems identification. The design challenge has principal parts, the first using a mathematical model, and the second using laboratory experimental apparatus. The specific parts of the Spacecraft Control Laboratory Experiment (SCOLE) program will be discussed in detail.

Control Objectives

The primary control task is to rapidly slew or change the line-of-sight of an antenna attached to the space Shuttle orbiter, and to settle or damp the structural vibrations to the degree required for precise pointing of the antenna. The objective will be to minimize the time required to slew and settle, until the antenna line-of-sight remains within the angle δ . A secondary control task is to change direction during the "on-target" phase to prepare for the next slew maneuver. The objective is to change attitude and stabilize as quickly as possible, while keeping the line-of-sight error less than δ .

Math Model Dynamics

The initial phase of the design challenge will use a mathematical model of the Shuttle orbiter/antenna configuration. It is necessary to obtain a balance, of course, between complex formulations which might be more accurate and simplified formulations which ease the burden of analysis.

The dynamics are described by a distributed parameter beam equation with rigid bodies, each having mass and inertia at either end. One body represents Space Shuttle orbiter; the other body is the antenna reflector. The equations for the structural dynamics and Shuttle motion are formed by adding to the rigid-body equations of motion, beam-bending and torsion equations. The boundary conditions at the ends of the beam contain the forces and moments of the rigid Shuttle and reflector bodies. The nonlinear kinematics couples the otherwise uncoupled beam equations. Additional terms represent the action of two, 2-axis proof-mass actuators at locations on the beam chosen by the designer.

The rigid-body equations of motion for the Shuttle body are given by:

$$\dot{\omega}_1 = - I_1^{-1} (\tilde{\omega}_1 I_1 \omega_1 + M_1 + M_D + M_{B,1})$$

$$\dot{v} = \frac{F_{B,1}}{m_1}$$

Similarly, for the reflector body,

$$\dot{\omega}_4 = -I_4^{-1}(\tilde{\omega}_4 I_4 \omega_4 + M_4 + M_{B,4})$$

$$\dot{v}_4 = \frac{F_4 + F_{B,4}}{m_4}$$

The direction cosine matrices defining the attitudes of the Shuttle and reflector bodies are given by:

$$\dot{T}_1^T = -\tilde{\omega}_1 T_1^T$$

$$\dot{T}_4^T = -\tilde{\omega}_4 T_4^T$$

The direction cosine matrices defining the attitudes of the Shuttle and the reflector bodies are related to the beam end conditions.

$$T_4 = \begin{bmatrix} 1 & 0 & 0 \\ 0 & \cos\Delta\phi & -\sin\Delta\phi \\ 0 & \sin\Delta\phi & \cos\Delta\phi \end{bmatrix} \begin{bmatrix} \cos\Delta\theta & 0 & \sin\Delta\theta \\ 0 & 1 & 0 \\ -\sin\Delta\theta & 0 & \cos\Delta\theta \end{bmatrix} \begin{bmatrix} \cos\Delta\psi & -\sin\Delta\psi & 0 \\ \sin\Delta\psi & \cos\Delta\psi & 0 \\ 0 & 0 & 1 \end{bmatrix} T_1$$

where:

$$\Delta\psi = u_\psi \Big|_{s=L} - u_\psi \Big|_{s=0}$$

$$\Delta\theta = \frac{\partial u_\theta}{\partial s} \Big|_{s=L} - \frac{\partial u_\theta}{\partial s} \Big|_{s=0}$$

$$\Delta\phi = \frac{\partial u_\phi}{\partial s} \Big|_{s=L} - \frac{\partial u_\phi}{\partial s} \Big|_{s=0}$$

The equations of motion for the flexible beam-like truss connecting the reflector and Shuttle bodies consist of standard beam bending and torsion partial differential equations with energy dissipative terms which enable damped modes with constant characteristics for fixed, though dynamic, end conditions. The system of equations can be viewed as driven by changing end conditions and forces applied at the locations of the proof-mass actuators.

ROLL BEAM BENDING:

$$PA \frac{\partial^2 u_\phi}{\partial t^2} - 2\zeta_\phi \sqrt{PA EI_\phi} \frac{\partial^3 u_\phi}{\partial s^2 \partial t} + EI_\phi \frac{\partial^4 u_\phi}{\partial s^4} = \sum_{n=1}^4 [f_{\phi,n} \delta(s-s_n) + g_{\phi,n} \frac{\partial \delta}{\partial s}(s-s_n)]$$

PITCH BEAM BENDING:

$$PA \frac{\partial^2 u_\theta}{\partial t^2} - 2\zeta_\theta \sqrt{PA EI_\theta} \frac{\partial^3 u_\theta}{\partial s^2 \partial t} + EI_\theta \frac{\partial^4 u_\theta}{\partial s^4} = \sum_{n=1}^4 [f_{\theta,n} \delta(s-s_n) + g_{\theta,n} \frac{\partial \delta}{\partial s}(s-s_n)]$$

YAW BEAM TORSION:

$$PI_\psi \frac{\partial^2 u_\psi}{\partial t^2} + 2\zeta_\psi I_\psi \sqrt{GP} \frac{\partial^3 u_\psi}{\partial s^2 \partial t} + GI_\psi \frac{\partial^2 u_\psi}{\partial s^2} = \sum_{n=1}^4 g_{\psi,n} \delta(s-s_n)$$

where:

$$f_{\phi,1} = m_1 \left. \frac{\partial^2 u_\phi}{\partial t^2} \right|_{s=0} \quad \{\text{SHUTTLE BODY FORCE}\}$$

$$f_{\phi,2} = m_2 \left. \frac{\partial^2 u_\phi}{\partial t^2} \right|_{s=s_2} + m_2 \frac{\partial^2 \Delta_{\phi,2}}{\partial t^2} \quad \{\text{PROOF-MASS ACTUATOR FORCE}\}$$

$$f_{\phi,3} = m_3 \left. \frac{\partial^2 u_{\phi}}{\partial t^2} \right|_{s=s_3} + m_3 \frac{\partial^2 \Delta_{\phi,2}}{\partial t^2} \quad \{\text{PROOF-MASS ACTUATOR}\}$$

$$f_{\phi,4} = m_4 \left. \frac{\partial^2 u_{\phi}}{\partial t^2} \right|_{s=130} - I_{zz,4} \frac{\partial^2 u_{\psi}}{\partial t^2} / 32.5 + F_y \quad \{\text{REFLECTOR BODY FORCE}\}$$

$$f_{\theta,1} = m_1 \left. \frac{\partial^2 u_{\theta}}{\partial t^2} \right|_{s=s_1} \quad \{\text{SHUTTLE BODY FORCE}\}$$

$$f_{\theta,2} = m_2 \left. \frac{\partial^2 u_{\theta}}{\partial t^2} \right|_{s=s_2} + m_2 \frac{\partial^2 \Delta_{\theta,2}}{\partial t^2} \quad \{\text{PROOF-MASS ACTUATOR FORCE}\}$$

$$f_{\theta,3} = m_3 \left. \frac{\partial^2 u_{\theta}}{\partial t^2} \right|_{s=s_3} + m_3 \frac{\partial^2 \Delta_{\theta,2}}{\partial t^2} \quad \{\text{PROOF-MASS ACTUATOR FORCE}\}$$

$$f_{\theta,4} = m_4 \left. \frac{\partial^2 u_{\theta}}{\partial t^2} \right|_{s=130} - I_{zz,4} \frac{\partial^2 u_{\psi}}{\partial t^2} / 18.75 - F_x \quad \{\text{REFLECTOR BODY FORCE}\}$$

$$\begin{pmatrix} g_{\phi,1} \\ g_{\theta,1} \\ g_{\psi,1} \end{pmatrix} = I_1 \dot{\omega}_1 + \omega_1 I_1 \omega_1 + M_1 + M_D$$

{SHUTTLE BODY, MOMENTS}

$$\begin{pmatrix} g_{\phi,2} \\ g_{\theta,2} \\ g_{\psi,2} \end{pmatrix} = 0$$

{PROOF-MASS ACTUATOR, MOMENT}

$$\begin{pmatrix} g_{\phi,3} \\ g_{\theta,3} \\ g_{\psi,3} \end{pmatrix} = 0$$

{PROOF-MASS ACTUATOR, MOMENT}

$$\begin{pmatrix} g_{\phi,4} \\ g_{\theta,4} \\ g_{\psi,4} \end{pmatrix} = I_4 \dot{\omega}_4 + \omega_4 I_4 \omega_4 + M_4 + \tilde{R}_B^F F_{B,4}$$

{REFLECTOR BODY, MOMENT}

The angular velocity of the reflector body is related to the Shuttle body by:

$$\omega_4 = \begin{pmatrix} \left. \frac{\partial^2 u_\phi}{\partial s \partial t} \right|_{s=L} \\ \left. \frac{\partial^2 u_\theta}{\partial s \partial t} \right|_{s=L} \\ \left. \frac{\partial u_\psi}{\partial t} \right|_{s=L} \end{pmatrix} - \begin{pmatrix} \left. \frac{\partial^2 u_\phi}{\partial s \partial t} \right|_{s=0} \\ \left. \frac{\partial^2 u_\theta}{\partial s \partial t} \right|_{s=0} \\ \left. \frac{\partial u_\psi}{\partial t} \right|_{s=0} \end{pmatrix} + \omega_1$$

$$\tilde{R}_B = \begin{bmatrix} 0 & 130 & 0 \\ -130 & 0 & 0 \\ 0 & 0 & 0 \end{bmatrix}$$

The line-of-sight error described in figure 2 is affected by both the pointing error of the Shuttle body and the misalignment of the reflector due to the deflection of the beam supporting the reflector. The line-of-sight is defined by a ray from the feed which is reflected at the center of the reflector. Its direction in the Shuttle body coordinates is given by:

$$R_{LOS} = \frac{-R_R + R_F + 2 \left[R_A^T (R_R - R_F) \cdot R_A \right]}{\left| \left| R_R - R_F - 2 \left[R_A^T (R_R - R_F) \cdot R_A \right] R_A \right| \right|}$$

where:

R_F is the feed location (3.75, 0, 0)

R_R is the location of the center of the reflector (18.75, -32.5, -130) *in an undeflected state*.

R_A is a unit vector in the direction of the reflector axis in Shuttle body coordinates

The vector R_A can be related to the direction cosine attitude matrices for the Shuttle body, T_1 , and the reflector body, T_4 , by

$$R_A = \begin{bmatrix} T_1^T T_4 \end{bmatrix} \begin{pmatrix} 0 \\ 0 \\ 1 \end{pmatrix}$$

The relative alignment of the reflector to the Shuttle body is given by

$T_1^T T_4$ which is a function of the structural deformations of the beam.

The line-of-sight error, e , is the angular difference between the target direction, given by the unit vector, D_T , and the line-of-sight direction in Earth axes, $T_1 R_{LOS}$.

$$e = \text{ARCSIN} \left| D_T \times T_1 R_{LOS} \right| \quad \text{or} \quad \text{ARCSIN} \left| \tilde{D}_T T_1 R_{LOS} \right|$$

Computer programs are available which generate time histories of the rigid body and the mode shapes and frequencies for the body-beam-body configuration for "pitch" bending, "roll" bending and "yaw" twisting. Since the modes are based on solving explicitly the distributed parameter equations (without damping and without kinematic coupling) there is no limit to the number of modal characteristic sets that can be generated by the program. It will be the analyst's decision as to how many modes need to be considered.

Laboratory Experiment Description

The second part of the design challenge is to validate in the laboratory, the system performance of the more promising control system designs of the first part. The experimental apparatus will consist of a dynamic model of the Space Shuttle orbiter with a large antenna reflector attached by means of a flexible beam. The dynamic model will be extensively instrumented and will have attached force and moment generating devices for control and for disturbance generation. A single, flexible tether will be used to suspend the dynamic model, allowing complete angular freedom in yaw, and limited freedom in pitch and roll. An inverted position will be used to let the reflector mast to hang so that gravity effects on mast bending will be minimized. The dynamics of the laboratory model will of necessity be different from the mathematical model discussed earlier.

Design Challenge, Part One

For part one of the design challenge, the following mathematical problem is addressed. Given the dynamic equations of the Shuttle/antenna configuration, what control policy minimizes the time to slew to a target and to stabilize so that the line-of-sight (LOS) error is held, for a time, within a specified amount, δ . During the time that the LOS error is within δ , the attitude must change 90° to prepare for the next slew maneuver. This was previously referred to as the secondary control task. The maximum moment and force generating capability will be limited. Advantage may be taken of selecting the most suitable initial alignment of the Shuttle/antenna about its assigned initial RF axis, line-of-sight. Random, broad band-pass disturbances will be applied to the configuration. Two proof-mass, force actuators may be positioned anywhere along the beam. The design guidelines are summarized below:

1. The initial line-of-sight error is 20 degrees.

$$e(o) = 20 \text{ degrees}$$

2. The initial target direction is straight down.

$$D_T = \begin{pmatrix} 0 \\ 0 \\ 1 \end{pmatrix}$$

3. The initial alignment about the line-of-sight is free to be chosen by the designer. Advantage may be taken of the low value of moment of inertia in roll. The Shuttle/antenna is at rest initially.
4. The objective is to point the line-of-sight of the antenna and stabilize to within 0.02 degree of the target as quickly as possible.

$$\delta = 0.02 \text{ degree}$$

5. Control moments can be applied at 100 Hz sampling rate to both the Shuttle and reflector bodies of 10,000 ft-lb for each axis. The commanded moment for each axis is limited to 10,000 ft-lb. The actual control moment's response to the commanded value is first-order with a time constant of 0.1 second.

For the rolling moment applied to the Shuttle body:

$$-10^4 \leq M_{X,1,\text{command}} \leq 10^4$$

$$M_{X,1}(n+1) = e^{-0.1} M_{X,1}(n) + (1 - e^{-0.1}) M_{X,1,\text{command}}(n)$$

Equations for other axes and for the reflector body are similar.

6. Control forces can be applied at the center of the reflector in the X and Y directions only. The commanded force in a particular direction is limited to 800 lbs. The actual control force's response to the commanded value is first-order with a response time of 0.1 second.

For the side force applied to the reflector body:

$$-800 \leq F_{Y,\text{command}} \leq 800$$

$$F_Y(n+1) = e^{-0.1} F_Y(n) + (1 - e^{-0.1}) F_{Y,\text{command}}(n)$$

Equations for X-axis are similar.

7. Control forces using two proof-mass actuators (each having both X and Y axes) can be applied at two points on the beam. The strokes are limited to ± 1 ft, and the masses weight 10 lbs each. The actual stroke follows a first-order response to limited commanded values.

For the X-axis of the proof-mass actuator at s_2 :

$$-1 \leq \Delta_{X,2,\text{command}} \leq 1$$

$$\Delta_{X,2}(n+1) = e^{-0.1} \Delta_{X,2}(n) + (1 - e^{-0.1}) \Delta_{X,2,\text{command}}(n)$$

Equations for other axes and locations are similar.

8. The inertial attitude direction cosine matrix for the Shuttle body lags in time the actual values by 0.01 second and are made at a rate of 100 samples per second. Each element of the direction cosine measurement matrix is contaminated by additive, uncorrelated Gaussian noise having an rms value of 0.001. The noise has zero mean.

$$T_{s,\text{measured}}(n+1) = T_{s,\text{true}}(n) + \begin{bmatrix} d_{11}(n) & d_{12}(n) & d_{13}(n) \\ d_{21}(n) & d_{22}(n) & d_{23}(n) \\ d_{31}(n) & d_{32}(n) & d_{33}(n) \end{bmatrix}$$

where:

$$E\{d_{ij}(n)\} = 0$$

$$E\{d_{ij}(n)d_{kL}(n)\} = 0 \quad \text{for } i \neq k \text{ or } j \neq L$$

$$E\{d_{ij}(n)d_{ij}(n+k)\} = 0 \quad \text{for } k \neq 0$$

$$= [0.001]^2 \quad \text{for } k = 0$$

9. The angular velocity measurements for both the Shuttle and reflector bodies pass through a first-order filter with 0.05 sec time constant and lag in time the actual values by 0.01 second and are made at a rate of 100 samples per second. Each rate measurement is contaminated by additive, Gaussian, uncorrelated noise having an rms value of 0.02 degree per second. The noise has zero mean.

For example:

$$\omega_{1,X,\text{measured}}^{(n+1)} = \omega_{1,X,\text{filtered}}^{(n)} + \epsilon_{1,X}^{(n)}$$

$$E\{\epsilon_{1,X}^{(n)} \epsilon_{1,X}^{(n+k)}\} = 0 \quad \text{for } k \neq 0$$

$$= (.02)^2 \quad \text{for } k = 0$$

where

$$\dot{\omega}_{1,X,\text{filtered}} = -20 \omega_{1,X,\text{filtered}} + 20 \omega_{1,X,\text{true}}$$

10. Three-axis accelerometers are located on the Shuttle body at the base of the mast and on the reflector body at its center. Two-axes (X and Y) accelerometers are located at intervals of 10 feet along the mast. The acceleration measurements pass through a first-order filter with a 0.05 second time constant and lag in time the actual values by 0.01 second, and are made at a rate of 100 samples per second. Each measurement is contaminated by Gaussian additive, uncorrelated noise having an rms value of 0.05 ft/sec².

For example:

$$a_{1,X,\text{measured}}^{(n+1)} = a_{1,X,\text{filtered}}^{(n)} + \tau_{1,X}^{(n)}$$

$$E\{\tau_{1,X}^{(n)} \tau_{1,X}^{(n+k)}\} = 0 \quad \text{for } k \neq 0$$

$$= (.05)^2 \quad \text{for } k = 0$$

where:

$$\dot{a}_{1,X,\text{filtered}} = -20 a_{1,X,\text{filtered}} + 20 \omega_{1,X,\text{true}}$$

11. Gaussian, uncorrelated step-like disturbances are applied 100 times per second to the Shuttle body in the form of 3-axes moments, having rms values of 100 ft-lbs. These disturbances have zero mean.

For example:

$$E\{M_{D,X}^{(n)} M_{D,X}^{(n+k)}\} = 0 \quad \text{for } k \neq 0$$

$$= (100)^2 \quad \text{for } k = 0$$

In summary, the designer's task for part one is to: (1) derive a control law for slewing and stabilization, coded in FORTRAN; (2) select an initial attitude in preparation for slewing 20 degrees; and (3) select two positions for the 2-axes proof-mass actuators. An official system performance assessment computer program will be used to establish the time required to slew and stabilize the Shuttle/antenna configuration.

Design Challenge, Part Two

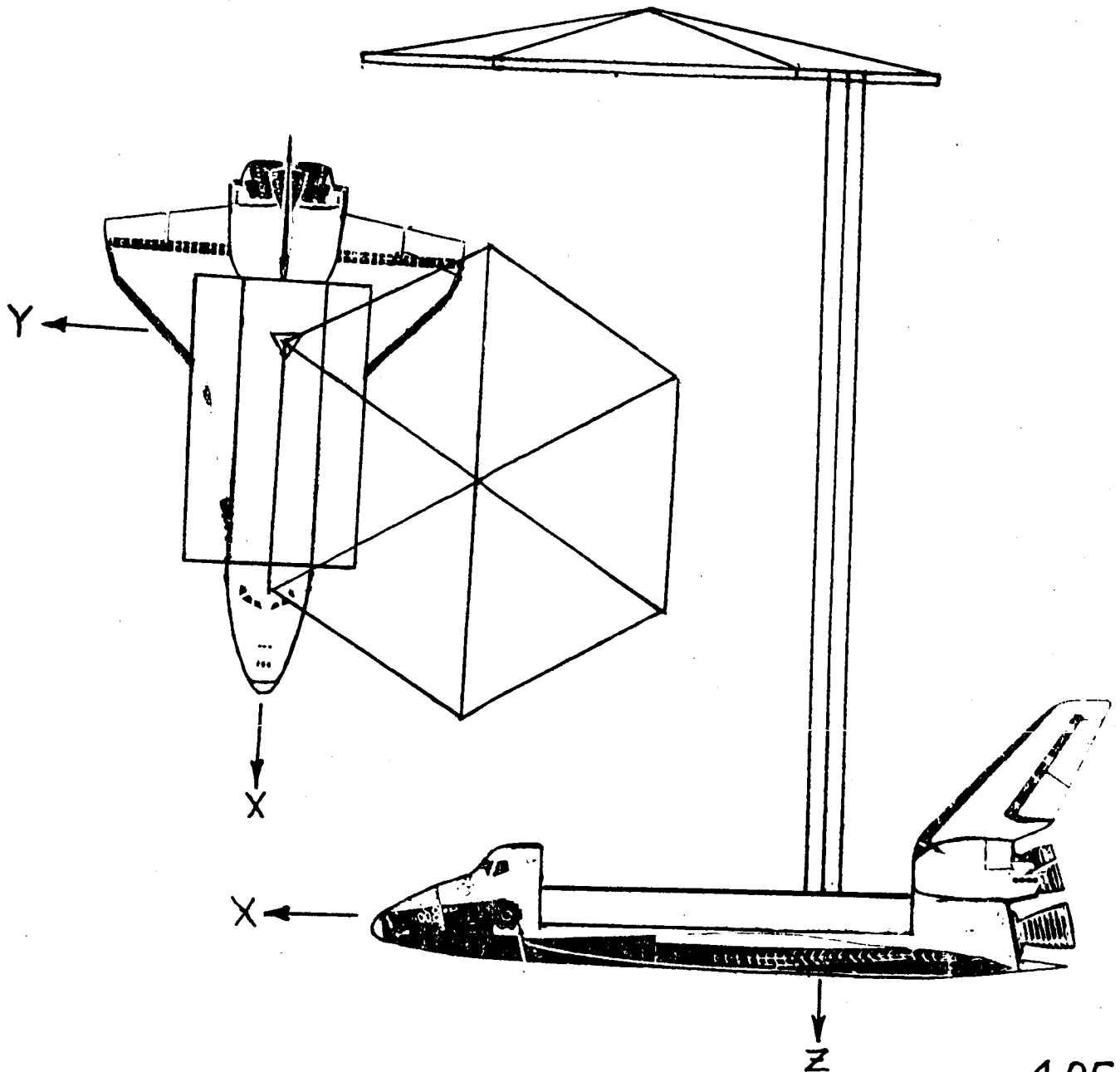
As in part one, the task is to minimize the time to slew and stabilize a Shuttle/antenna configuration. The difference is that in part two of the design challenge, a physical laboratory model will be used instead of the dynamic equations of part one. The constraints on total moment and force generation capability will apply to part two, as for part one. Again, the analyst may select the initial alignment about the assigned initial RF line-of-sight. Disturbances will be injected into the Shuttle/antenna model. The designer's task will be similar to that for part one.

CONCLUDING REMARKS

A Design Challenge, in two parts, has been offered for the purpose of comparing directly different approach to controlling a flexible Shuttle/antenna configuration. The first part of the design challenge uses only mathematical equations of the vehicle dynamics; the second part uses a physical laboratory model of the same configuration. The Spacecraft Control Laboratory Experiment (SCOLE) program is being conducted under the cognizance of the Spacecraft Control Branch at the NASA Langley Research Center. The NASA/IEEE Design Challenge has the advice and counsel of the IEEE-COLSS Subcommittee on Large Space Structures. Workshops will be held to enable investigators to compare results of their research.

Figure 1. Drawing of the Shuttle/Antenna Configuration.

SPACECRAFT CONTROL LAB EXPERIMENT (SCOLE)



CRITICAL MOMENT OF ROTATION

The moment of inertia becomes:

$$I = \begin{bmatrix} I_{xx} & -I_{xy} & -I_{xz} \\ -I_{xy} & I_{yy} & -I_{yz} \\ -I_{xz} & -I_{yz} & I_{zz} \end{bmatrix} = \begin{bmatrix} 1,132,508 & 7,555 & -115,202 \\ 7,555 & 7,007,447 & -52,293 \\ -115,202 & -52,293 & 7,113,962 \end{bmatrix}$$

$$I_1 = \begin{bmatrix} 905,443 & 0 & -145,393 \\ 0 & 6,789,100 & 0 \\ -145,393 & 0 & 7,086,601 \end{bmatrix}$$

$$I_4 = \begin{bmatrix} 4,969 & 0 & 0 \\ 0 & 4,969 & 0 \\ 0 & 0 & 9,938 \end{bmatrix}$$

$$m = 6391.30 \text{ slugs}$$

$$m_1 = 6366.46 \text{ slugs}$$

$$m_2 = 0.3108 \text{ slugs}$$

$$m_3 = 0.3108 \text{ slugs}$$

$$m_4 = 12.42 \text{ slugs}$$

$$PA = 0.09556 \text{ slugs/ft}$$

$$I_\phi = 4.0 \times 10^7 \text{ lb-ft}^2$$

$$= .003$$

$$= 0.9089 \text{ slug-ft}$$

$$= 4.0 \times 10^7 \text{ lb-ft}^2$$

$$= .003$$

$$PA = 0.09556 \text{ slugs/ft}$$

$$EI_\theta = 4.0 \times 10^7 \text{ lb-ft}^2$$

$$\zeta_\theta = .003$$

MASS CHARACTERISTICS

| | CG LOCATION, FT | | | WEIGHT, LB | I_{XX}^2 SLG-FT ² | I_{YY}^2 SLG-FT ² | I_{ZZ}^2 SLG-FT ² | I_{XY}^2 SLG-FT ² | I_{XZ}^2 SLG-FT ² | I_{YZ}^2 SLG-FT ² |
|-----------------------------------|-------------------|-------|-------|------------|-----------------------------------|-----------------------------------|-----------------------------------|-----------------------------------|-----------------------------------|-----------------------------------|
| | X | Y | Z | | | | | | | |
| SHUTTLE | 0 | 0 | 0 | 205,000 | 905,443 | 6,789,100 | 7,086,601 | 0 | 145,393 | 0 |
| MAST, CG | 0 | 0 | -65. | 400 | 17,495 | 17,495 | 0 | 0 | 0 | 0 |
| REFLECTOR, CG | 18.75 -32.5 -130. | | | 400 | 4,969 | 4,969 | 9,938 | 0 | 0 | 0 |
| REFLECTOR, ATTACHMENT POINT | | | | | 18,000 | 9,336 | 27,407 | -7,570 | 0 | 0 |
| TOTAL | .036 | -.063 | -.379 | 205,800 | 1,132,508 | 7,007,447 | 7,113,962 | -7,555 | 115,202 | 52,293 |

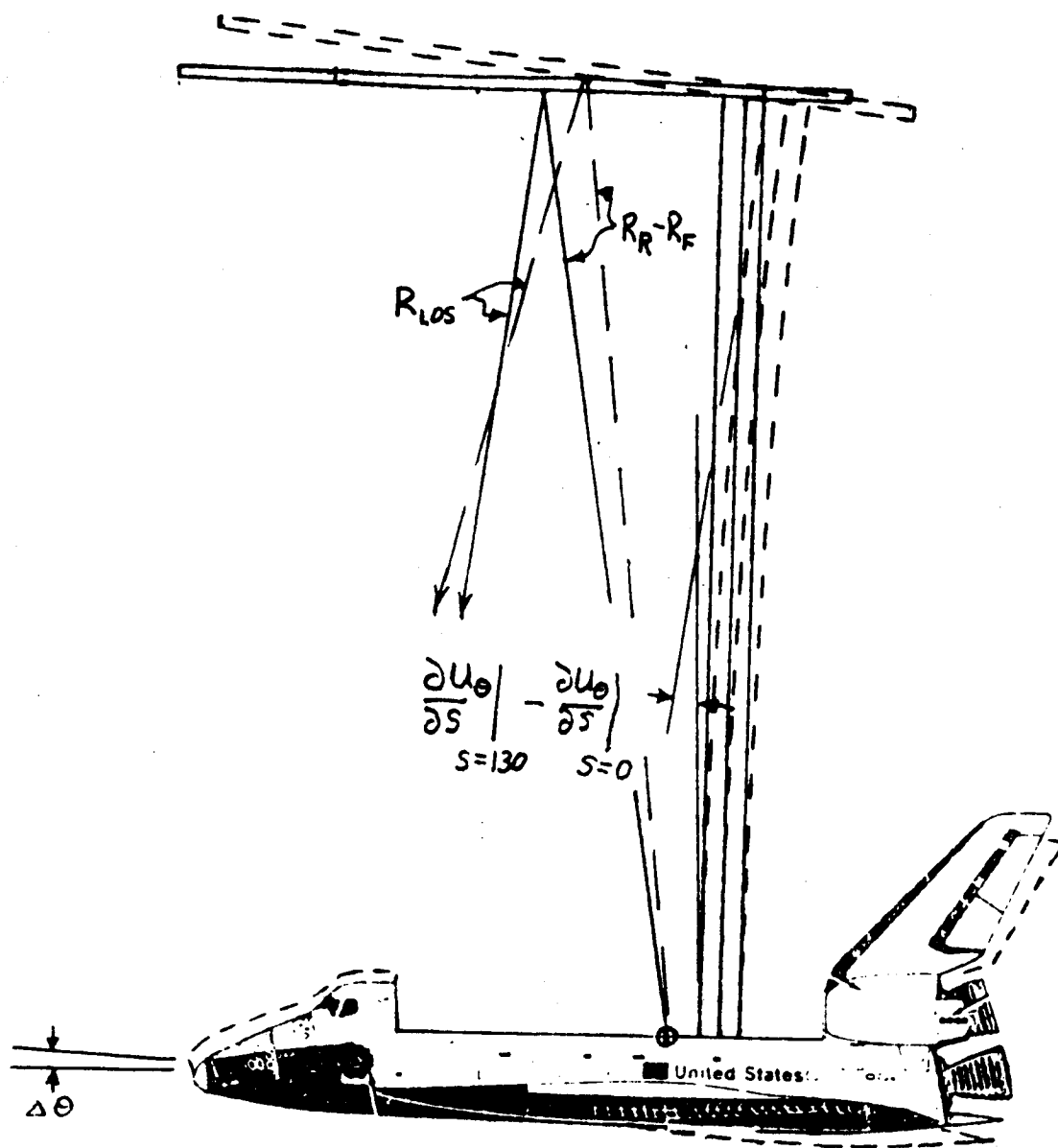
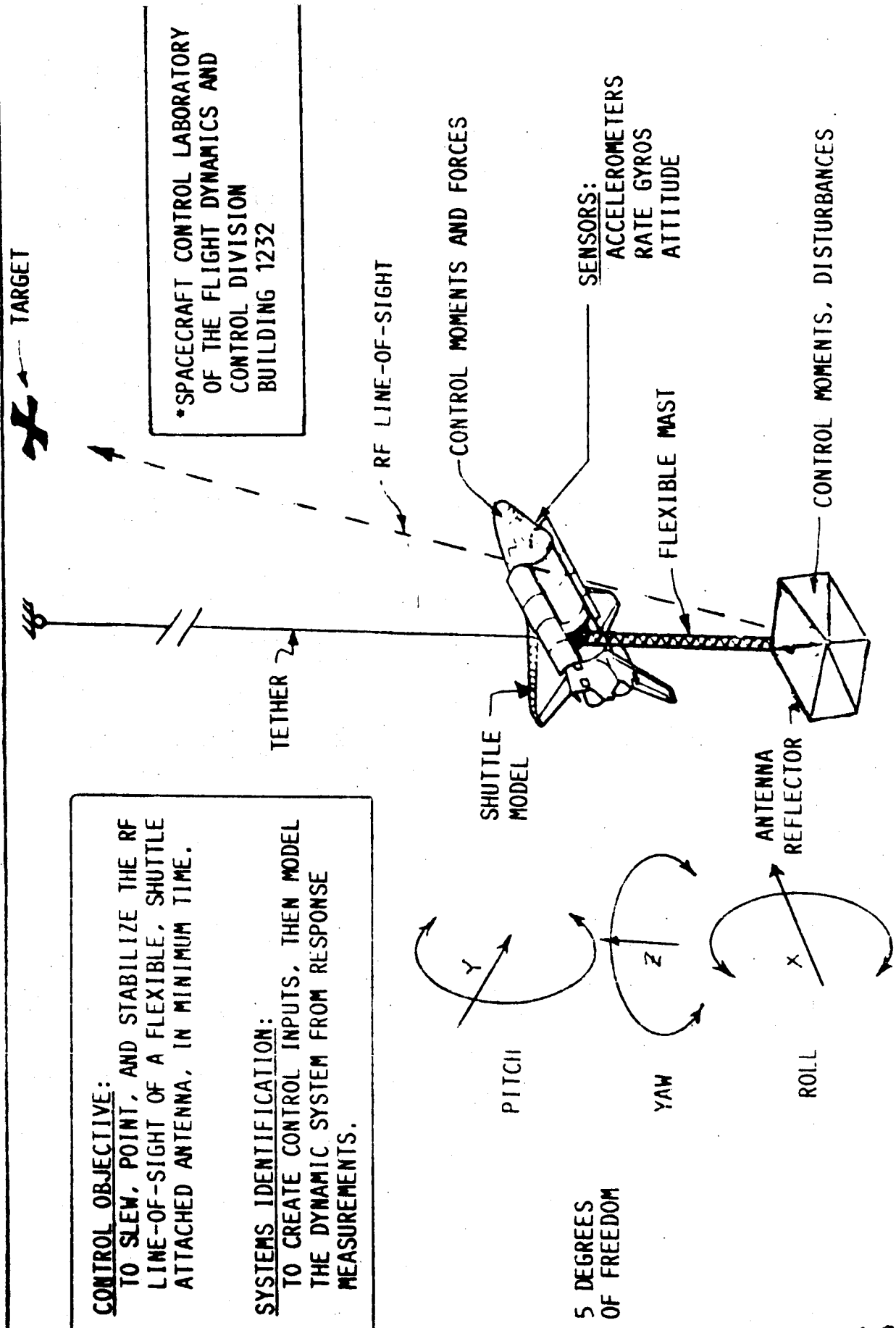


Figure 2.- Schematic of the effect of bending on the line-of-sight pointing error.

Figure 3. SPACECRAFT CONTROL LABORATORY* EXPERIMENT (SCOLE)



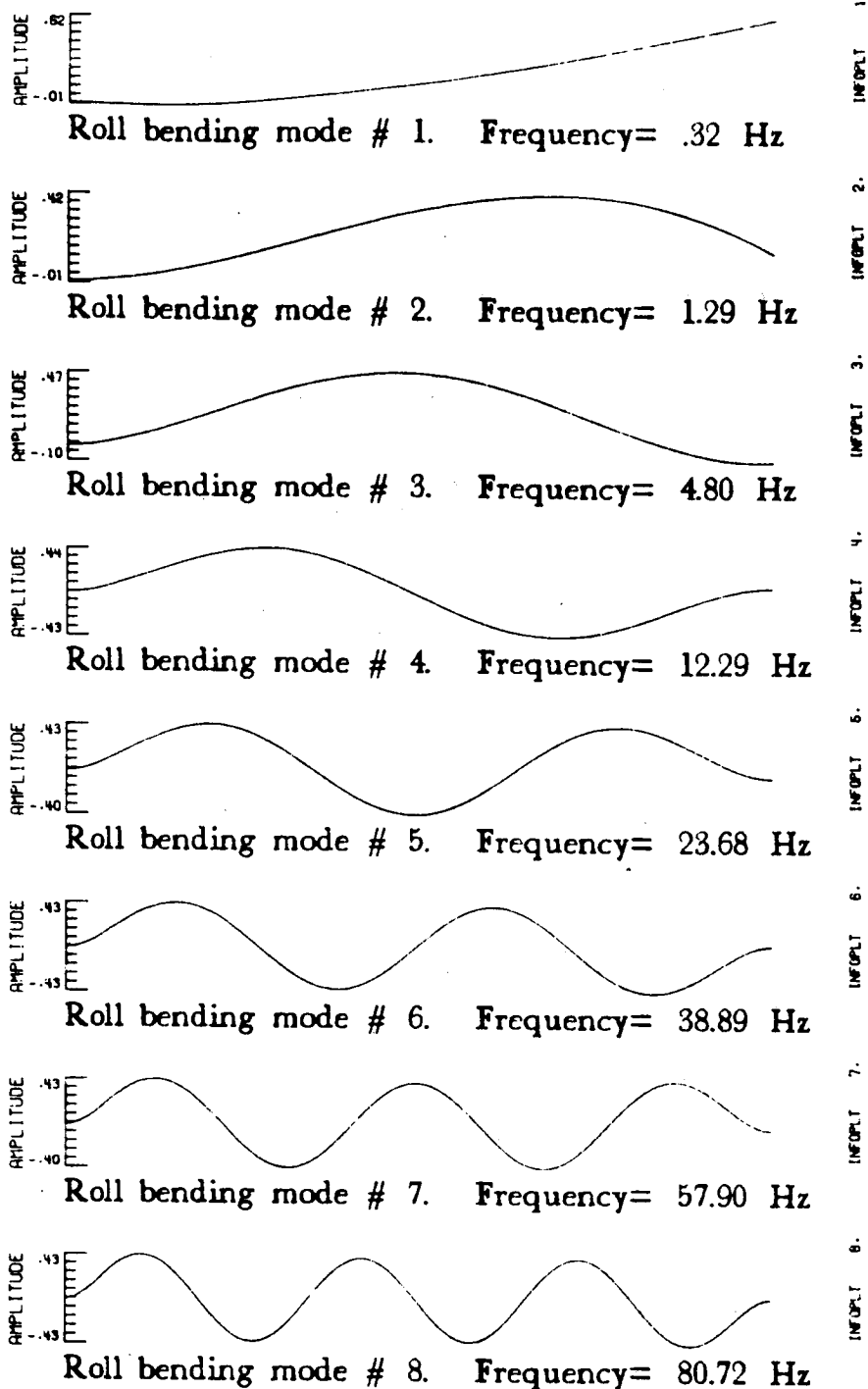


Figure 4a.- Plots of normalized roll bending mode shapes for SCOLE configuration.

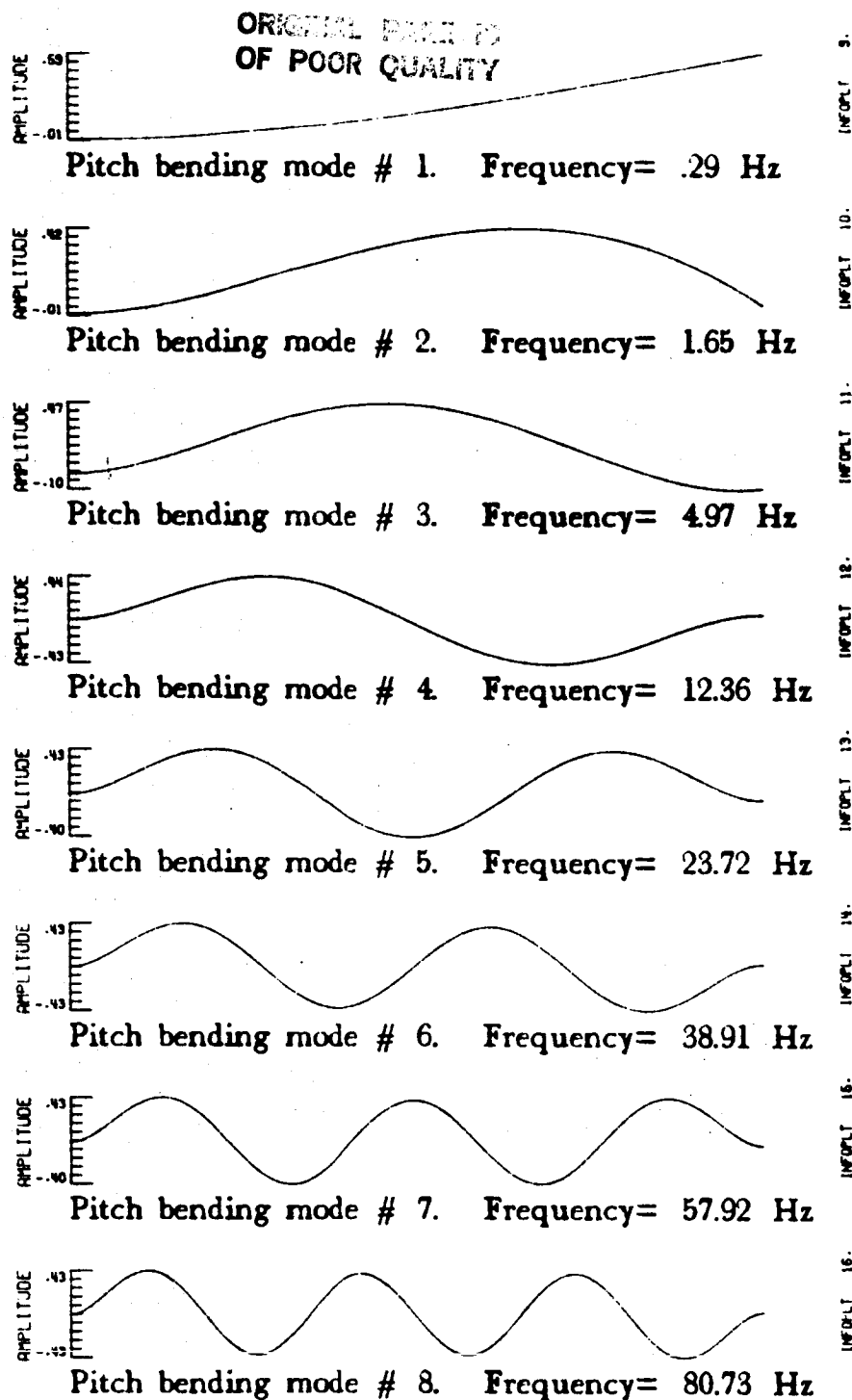


Figure 4b.- Plots of normalized pitch bending mode shapes for SCOPE configuration.

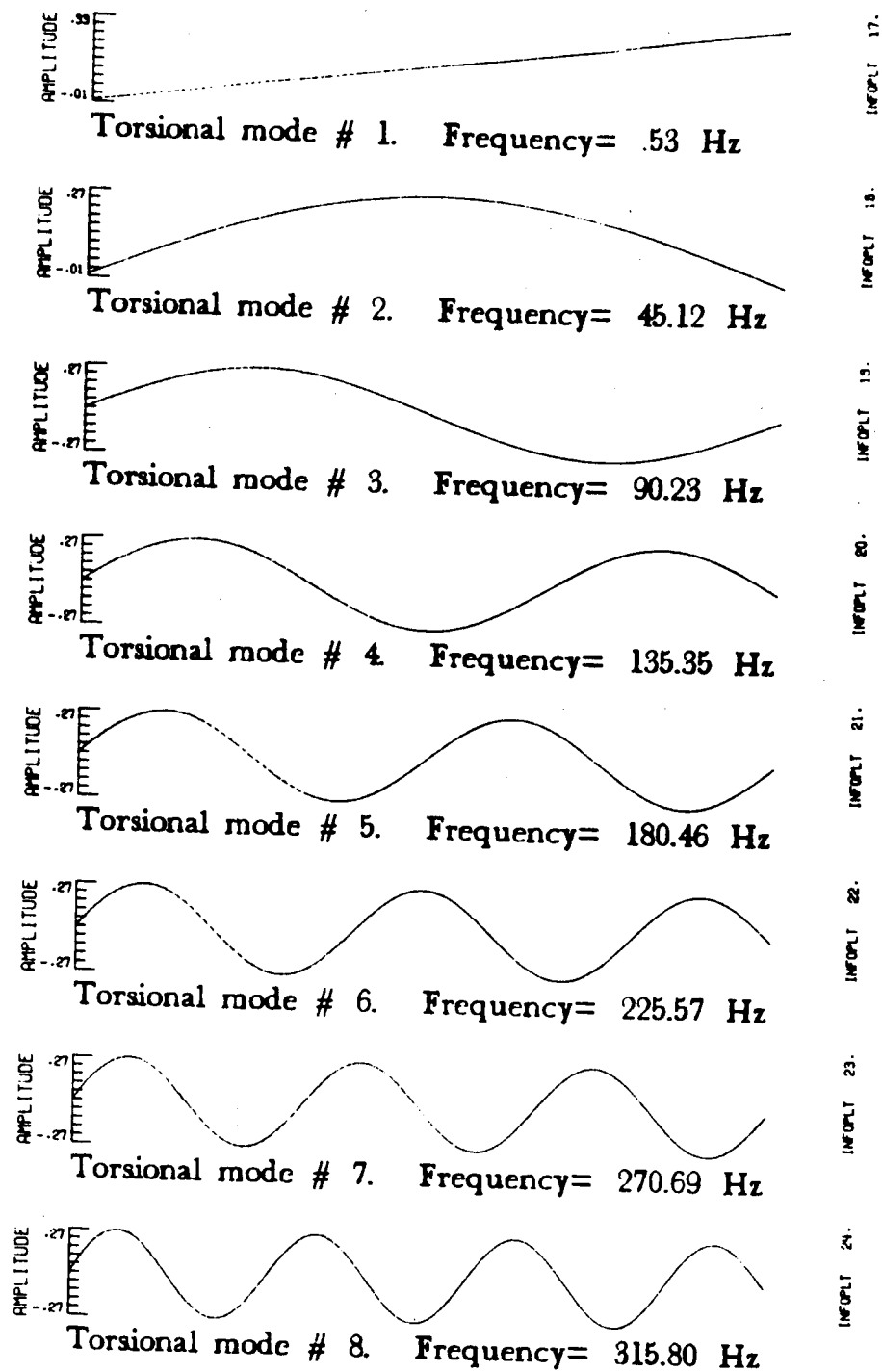


Figure 4c.- Plots of normalized torsional mode shapes for SCOPE configuration.